

New measurements of the proton's size and structure using polarized photons

J. Arrington

Physics Division, Argonne National Laboratory, Argonne, IL 60439

Abstract.

Improved measurements of the proton's structure are now possible thanks to significant technical advances that allow us to probe the proton with *polarized* photons. These measurements have shown that the proton is not as simple as previously believed: quark orbital angular momentum and relativistic effects play an important role and the spatial distribution of charge and magnetization do not simply mimic the spatial distribution of the quarks. Even more recently, the large scale structure and size of the proton have been examined more carefully, and a significant discrepancy has been observed between the charge radius of the proton as measured in the Lamb shift of muonic hydrogen and measurements using the electron–proton interaction.

Keywords: nucleon electromagnetic form factors, charge radius, elastic scattering

PACS: 13.40.Gp, 14.20.Dh, 25.30.Bf

While the proton and neutron are thought of as the basic building blocks of visible matter, they are, in fact, complicated bound states of quarks and gluons, held together by the strong interactions described by Quantum Chromodynamics (QCD). The forces binding quarks together are so powerful that it is impossible to simply pluck a single quark from a proton; attempting to do so requires energies so large that new quarks and gluons are “ripped” out of the vacuum, forming new bound states (hadrons) around the quark one is attempting to isolate. Therefore, studying the interactions of QCD involves careful examination of the internal structure of *bound states* of quarks to isolate information that is directly sensitive to the underlying quark degrees of freedom. Because of this, the proton plays an important dual role as both a basic building block of visible matter and the most accessible bound state of QCD, and as such, has been a primary focus for generations of nuclear physicists.

In the last several years, new experimental tools have led to unprecedented improvements in our ability to study the internal structure of the proton and neutron. Measurements utilizing polarized electron beams allow the proton to be probed with polarized virtual photons, and the comparison of spin-flip and non-spin-flip interactions provides access to small and difficult to measure components of the protons electromagnetic structure. These measurements have been made possible by advances in high-current, high-polarization electron beams along with improved polarized targets and recoil polarimeters. These techniques are now in common usage at Jefferson Lab (JLab) after pioneering work at SLAC, BATES, and Mainz [1, 2, 3].

The distributions of the proton's charge and magnetization are encoded in the elastic electromagnetic form factors, which are measured in elastic electron–proton scattering. The elastic e–p scattering cross section depends on the two elastic form factors, $G_E(Q^2)$ and $G_M(Q^2)$, which depend only on the square of the four-momentum transfer, and

which describe the difference between scattering from a structureless particle and an extended, complex object. By measuring the form factors, we probe the spatial distribution of the proton charge and magnetization, providing the most direct connection to the spatial distribution of quarks inside the proton. In the non-relativistic limit, the form factors are simply Fourier transforms of the charge and magnetization spatial densities. The size of the proton is related to the strength of the forces that bind quarks and gluons together, while the detailed distributions provide information on the quark dynamics, and yield strong constraints on models of the proton internal structure.

In electron scattering, the electron interacts with the proton via exchange of a virtual photon, characterized by its momentum transfer, Q^2 . At low Q^2 , the long wavelength photon is sensitive to the size and large scale structure of the proton, while at high Q^2 , the photon probes the fine details of the structure, as illustrated in Figure 1 (left panel). In the Born (single photon exchange) approximation, the elastic e-p cross section is proportional to the reduced cross section, $\sigma_R = [(Q^2/4m^2)G_M^2(Q^2) + \epsilon G_E^2(Q^2)]$, where m is the proton mass, θ is the electron scattering angle, and $\epsilon^{-1} = 1 + 2(1 + Q^2/4m^2) \tan^2(\theta/2)$. The presence of the angle-dependent factor ϵ multiplying G_E allows a Rosenbluth separation [4] of the form factors by examining the ϵ dependence of σ_R at fixed Q^2 .

For over 50 years, extractions of the form factors using the Rosenbluth technique appeared to show that the normalized charge and magnetic form factors were approximately equal for the proton, and were similar to the magnetic form factor of the neutron. This is consistent with non-relativistic quark models of the proton and neutron structure, where the nucleon's charge and magnetization are simply carried by the quarks, with identical spatial distributions for up and down quarks. The only deviation from this simple picture was the small, non-zero result for the electric form factor of the neutron. This indicated a small difference between the up and down quark distributions, since identical spatial densities for up and down quarks would yield perfect cancellation of their charges at all points in space, resulting in a vanishing electric form factor.

Because the cross section is proportional to a combination of two terms, it is difficult to extract one form factor when the other dominates the cross section, limiting extractions of G_M at very low Q^2 and G_E at very high Q^2 . This difficulty led to interest in polarization measurements which depend only on the *ratio* G_E/G_M , but which require polarized electron beams and either polarized targets or proton recoil polarimeters. Combining cross section and polarization measurements allows a clean extraction of both form factors, even where one is strongly suppressed in the cross section. With the new polarization techniques, it has become possible to study in much greater detail the charge and magnetization distributions. This allows us to look for deviations from our simple picture, and to more carefully examine contributions that yield differences between up- and down-quark distributions, such as the “pion cloud” of the nucleon [5], illustrated in Fig. 1 (right panel). With the inclusion of parity violating elastic scattering, it is also possible to isolate the contribution of strange quarks to the proton form factors [6, 7], given sufficiently precise knowledge of the up- and down-quark contributions to make a reliable extraction of the strange-quark contribution.

One of the biggest surprises of the JLab form factor program was the falloff of G_E/G_M at high Q^2 [8, 9, 10], which was at odds with decades of cross section measurements [11]. The high- Q^2 polarization data indicates that the ratio of electric to mag-

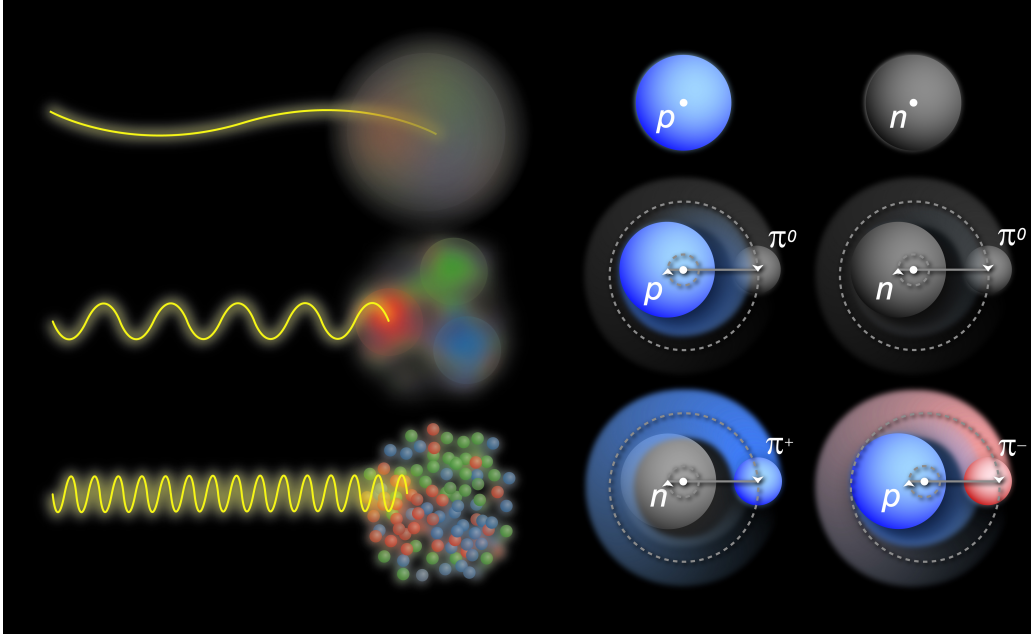


FIGURE 1. **Left:** Illustration of the structure probed in electron–proton scattering at various energy scales. At low energy, the virtual photon probes the proton at large distance scales and is sensitive to the size and large-scale structure. At higher energies, the photons probe shorter distance scales, probing the constituent quarks or the sea of quark-antiquark pairs. **Right:** Illustration of the impact of the “pion cloud” to the charge distribution of the proton (left) and neutron (right) charge radii. Blue (red) indicates positive (negative) charge, and presence of a virtual pion–nucleon has two main effects. First, the motion of the system yields a ‘smearing’ of the nucleon charge distribution due to its center-of-mass motion. Second, the charge pion associated with the $n \rightarrow p + \pi^-$ fluctuation yields a negative contribution at large distances. *Credit: Joshua Rubin, Argonne National Laboratory*

netic form factors is constant at very low Q^2 , then falls almost linearly with Q^2 , as shown in Figure 2. This contradicted previous measurements which showed $\mu_p G_E/G_M \approx 1$, in agreement with the simple non-relativistic model. The difference between the polarization and cross section extractions is now believed to be the result of two-photon exchange contributions. These have little impact on polarization measurements but significantly affect Rosenbluth extractions of G_E at high Q^2 , making it appear as though $\mu_p G_E/G_M \approx 1$ [12, 13, 14, 15]. Definitive tests of the effect on the cross sections using precise comparisons of positron and electron scattering are currently under way [16].

While this decrease of $\mu_p G_E/G_M$ with Q^2 was largely unexpected, it is perhaps not so surprising that relativistic effects become important at these large momenta, and that the predictions of non-relativistic models break down. These results led to an explosion of theoretical interest in trying to understand the proton form factors [1, 2]. The difference in the Q^2 dependence of G_{Ep} and G_{Mp} suggests a significant difference in the charge and magnetization densities of the proton [27], although one avoids model-dependent corrections only when working in the infinite-momentum frame [28, 29, 30]. While calculations which reproduce the falloff of G_E/G_M explain the effect in somewhat different terms [24, 25, 31, 32, 26], most of these link the effect directly or indirectly to significant contributions from quark orbital angular momentum [33, 34, 35]. In addition,

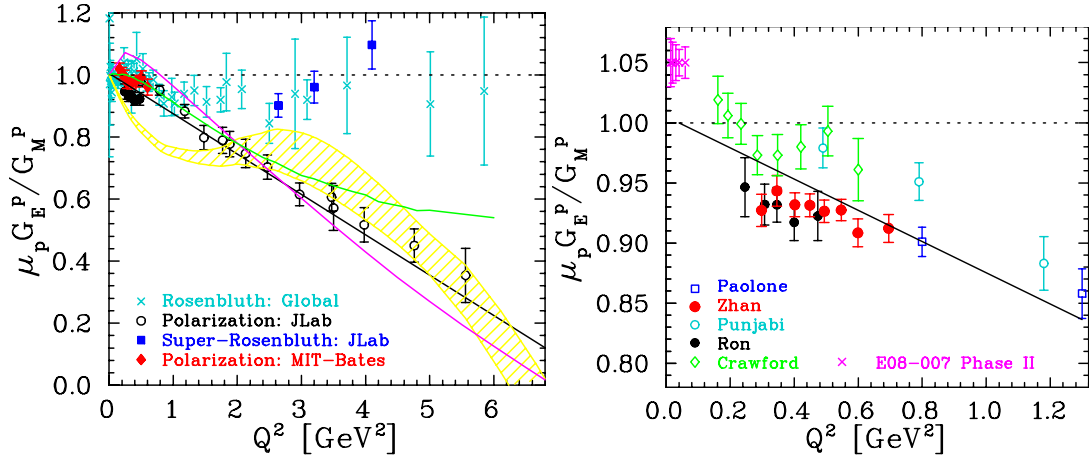


FIGURE 2. **Left:** The proton form factor ratio $\mu_p G_E^p / G_M^p$ from Rosenbluth measurements [11, 17, 18] (neglecting TPE corrections) and polarization measurements [8, 9, 19, 10, 20, 21, 22, 23]. The black curve is the fit from Ref [14], the magenta curve is the calculation of Ref. [24], the green curve is the calculation of Ref. [25], and the yellow band is the prediction of Ref. [26]. The precise polarization data show a rapid drop with Q^2 , while the Rosenbluth data are, on average, consistent with unity. **Right:** Polarization measurements of the ratio at low Q^2 along with the projected uncertainties for Phase II of JLab E08-007, which recently completed data taking.

interpretation of these results in terms of generalized parton distributions led to studies of the correlation between the spatial distribution of the quarks and the spin or momentum that they carry, showing that the spherically symmetric distribution of the proton is formed from a rich collection of complex overlapping structures [28, 29, 30, 36, 37, 38].

Recent measurements of the neutron charge form factor at Q^2 values up to 3.4 GeV^2 [39] allow for more detailed examination of the up- and down-quark contributions [40], showing significant difference between the quark contributions to F_1 and F_2 . For the up quarks, the form factors appear to fall as Q^{-4} above $Q^2=1.5 \text{ GeV}^2$, while the down quarks decrease as Q^{-2} . One interpretation of this is the importance of the quark-diquark structure of the proton, with the more strongly bound scalar (u-d) diquarks yielding a significant difference in the high- Q^2 behavior of the up- and down-quark contributions [41, 42]. The combination of precise measurements on the proton and the neutron at high- Q^2 , including recent measurements of G_{Mn} [43], also allows us to test models of the nucleon against a complete set of form factor measurements covering a wide range of momentum transfers. As different models make varied assumptions about the most relevant symmetries and degrees of freedom of QCD, this improves our ability to identify the aspects of the underlying physics that are most critical in determining the proton structure. Such studies will be further extended with the JLab 12 GeV upgrade [44], with the additional advantage that higher Q^2 studies will be less sensitive to pion cloud contributions, which are often added to the three-quark core in more simplified approximations.

As illustrated by the examples above, the measurements at large momentum transfer have provided significant new information on the details of the proton structure, including the importance of relativity, quark angular momentum, and the flavor structure of the

proton. By going to lower momentum transfer and thereby utilizing longer wavelength probes, we become sensitive to the size of the proton. This is the region where one expects to see the impact of the “pion cloud” of the proton, which arises from brief fluctuations of the proton into a bound system of a proton or neutron and pion, illustrated in Fig. 1. Because of the nucleon-pion mass difference, the nucleon will be located nearer the center of mass, and the pion will contribute at large distances. So the proton- π^0 contribution yields a small “blurring” of the intrinsic proton charge, due to the motion of the proton relative to the proton- π^0 center of mass, while the neutron- π^+ configuration contributes to the charge distribution at larger distances. This effect is most clear in the neutron electric form factor, which would be extremely small in the absence of such effects, and where the contribution from fluctuations into bound proton- π^- yields a positive core and a negative pion cloud. A recent analysis [5] showed suggestions of a similar structure in the proton form factors.

With precise new data in the low Q^2 region, is possible to better examine the form factors for indications of structure related to the pion cloud and to improve extractions of the proton charge and magnetic radii. A series of low Q^2 polarization measurements [19, 45, 23, 22, 21], the most recent of which achieved $\approx 1\%$ total uncertainties on $\mu_p G_E/G_M$ for Q^2 from 0.3 – 0.7 GeV². This is to be compared to typical uncertainties of 3–5% from earlier cross section measurements, and $\gtrsim 2\%$ for the previous low- Q^2 polarization measurements. Figure 2 shows the results of these recent polarization experiments, which have dramatically improved the precision of our knowledge of the form factor ratio $\mu_p G_E/G_M$ at low Q^2 . In addition, a new set of high-precision Rosenbluth measurements, focusing on Q^2 values below 1 GeV², have been taken at Mainz [46] and are in good agreement with the recent polarization data. While the Rosenbluth results are more sensitive to TPE contributions, TPE effects are generally expected to be smaller, at the $\sim 1\%$ level, at these Q^2 values [47, 48]. Nonetheless, these corrections can still impact the extracted radii [49, 50, 51].

Note that the new data on G_E/G_M rule out the kind of structure suggested in the analysis of previous data [5], although this does not mean that the contribution from the pion cloud are small. There could be significant structure that cancels in the form factor ratio, or there could be large pion cloud contributions which do not introduce any sort of “bump” or other clear structure in the form factors. The ratio $\mu_p G_E/G_M$ is significantly below unity over most of the measured range, with some uncertainty at the lowest Q^2 values due to a small inconsistency between the measurements in this region. However, the more precise polarization data, as well as the Mainz Rosenbluth results, indicate $\mu_p G_E/G_M < 1$, suggesting that the electric form factor falls off more rapidly than the magnetic form factor at low Q^2 . If this holds down to $Q^2=0$, it implies that the charge distribution is larger than the magnetization distribution. If this is the case, then there is *no energy scale at which the simple non-relativistic picture, where the quark, charge, and magnetization distributions are identical, is valid*. Even when probed at the lowest momentum scales, we are sensitive to the quark dynamics and the impact of the electric and magnetic fields generated by the motion of the highly-relativistic quarks.

The new data also provide updated extractions of the proton charge and magnetic RMS radii. In the non-relativistic limit, $G_E = 1 - Q^2 \langle r^2 \rangle / 6 + \dots$, allowing for the extraction of the mean-square radius, $\langle r^2 \rangle$, of the proton from the slope of the form factor

at $Q^2 = 0$. While the relativistic case yields corrections to this approximation, the slope of the form factor is taken as the standard definition used in all extractions of the proton charge radius. The analysis combining polarization data with previous cross section measurements yields a charge radius of 0.875(10) fm [21], consistent with the Mainz extraction of 0.879(8) fm [46] and the 2010 CODATA value of 0.878(5) fm [52], which is mainly derived from the Lamb shift in hydrogen. The finite size of the proton yields one of the largest corrections to the atomic structure of hydrogen, allowing precise measurements of the Lamb shift to be used as a measure of the proton charge radius.

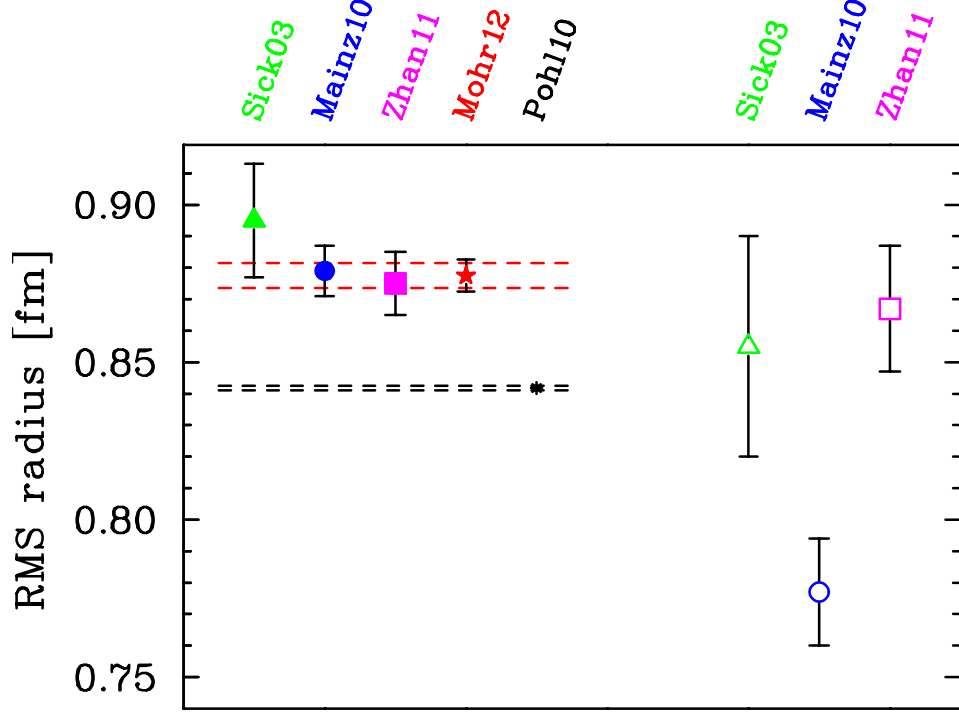


FIGURE 3. The proton RMS charge radius (solid points) and magnetic radius (hollow points) from electron scattering [53, 46, 21] and atomic physics [52, 54] measurements. The red dashed lines show the combined charge radius result from the electron-based CODATA, Bernauer, and Zhan extractions (Sick is excluded as Zhan includes the same data), while the black dashed lines show the Pohl uncertainty.

A recent measurement of the Lamb shift in muonic hydrogen [54] yields a proton RMS radius of 0.8418(07) fm, at odds with the electron scattering results and the CODATA10 [52] value of 0.8775(51) fm. These measurements of the proton charge radius are shown in Fig. 3. The combined extraction based on electron–proton interactions are consistent, and the combined result from these three measurements is $R_E=0.8772(46)$, 9σ above the muonic hydrogen result. The corrections applied to e–p scattering and to the atomic hydrogen Lamb shift are very different, and the agreement of the electron-based measurements suggests that the difference lies in the muonic hydrogen result, either related to the measurement of the Lamb shift, or the calculation of the QED corrections. Note that while there are concerns about the effect of two-photon exchange in extraction of the radius [49, 22, 50], the impact of these corrections appears to be small for the charge radius, but may account for some of the discrepancy between the magnetic radii extracted in the electron scattering measurements [51].

With the use of new polarization techniques, our picture of the proton is rapidly coming into much sharper focus, answering many questions about the structure of the proton. Recent high- Q^2 polarization measurements demonstrated the possible importance of two-photon exchange corrections and found clear indications of the key role of orbital angular momentum and quark dynamics in the proton structure. At low Q^2 , our new polarization data show a clear breakdown of non-relativistic quark models even at low momentum scales and provide evidence of a difference in the size of the proton's charge and magnetization distributions.

These measurements have raised new questions as well: are the two-photon exchange corrections observed at high Q^2 also yielding differences between new cross section and polarization measurements at very low momentum transfer, and do they, or other corrections, explain the difference between various extractions of the proton's charge radius. In the absence of an error in the measurement or QED corrections, this significant discrepancy indicates that something is missing in our description of the electromagnetic interaction which yields a difference between electron and muon interactions. If the difference between the proton radius obtained in e-p and μ -p interactions survives a more detailed examination, does this imply that something is missing in our description of the hydrogen atom or in our understanding of electron and muon interactions with matter?

This work was supported by the U.S. Department of Energy, Office of Nuclear Physics, under contract DE-AC-06CH11357

REFERENCES

1. C. F. Perdrisat, V. Punjabi, and M. Vanderhaeghen, *Prog. Part. Nucl. Phys.* **59**, 694–764 (2007).
2. J. Arrington, C. D. Roberts, and J. M. Zanotti, *J. Phys.* **G34**, S23 (2007).
3. J. Arrington, K. de Jager, and C. F. Perdrisat, *J. Phys. Conf. Ser.* **299**, 012002 (2011).
4. M. N. Rosenbluth, *Phys. Rev.* **79**, 615 (1950).
5. J. Friedrich, and T. Walcher, *Eur. Phys. J. A* **17**, 607–623 (2003).
6. D. H. Beck, and R. D. McKeown, *Ann. Rev. Nucl. Part. Sci.* **51**, 189–217 (2001).
7. D. Armstrong, and R. McKeown (2012), [arXiv:1207.5238](#).
8. V. Punjabi, et al., *Phys. Rev. C* **71**, 055202 (2005).
9. O. Gayou, et al., *Phys. Rev. Lett.* **88**, 092301 (2002).
10. A. J. R. Puckett, et al., *Phys. Rev. Lett.* **104**, 242301 (2010).
11. J. Arrington, *Phys. Rev. C* **68**, 034325 (2003).
12. P. A. M. Guichon, and M. Vanderhaeghen, *Phys. Rev. Lett.* **91**, 142303 (2003).
13. J. Arrington, *Phys. Rev. C* **69**, 022201(R) (2004).
14. J. Arrington, W. Melnitchouk, and J. A. Tjon, *Phys. Rev. C* **76**, 035205 (2007).
15. J. Arrington, P. Blunden, and W. Melnitchouk, *Prog. Part. Nucl. Phys.* **66**, 782–833 (2011).
16. J. Arrington, *AIP Conf. Proc.* **1160**, 13–18 (2009), [arXiv:0905.0713](#).
17. M. E. Christy, et al., *Phys. Rev. C* **70**, 015206 (2004).
18. I. A. Qattan, et al., *Phys. Rev. Lett.* **94**, 142301 (2005).
19. C. Crawford, et al., *Phys. Rev. Lett.* **98**, 052301 (2007).
20. A. Puckett, E. Brash, O. Gayou, M. Jones, L. Pentchev, et al., *Phys. Rev. C* **85**, 045203 (2012).
21. X. Zhan, et al., *Phys. Lett. B* **705**, 59–64 (2011).
22. G. Ron, et al., *Phys. Rev. C* **84**, 055204 (2011).
23. M. Paolone, et al., *Phys. Rev. Lett.* **105**, 072001 (2010).
24. M. Frank, B. Jennings, and G. Miller, *Phys. Rev. C* **54**, 920–935 (1996).
25. F. Cardarelli, and S. Simula, *Phys. Rev. C* **62**, 065201 (2000).
26. A. Holl, R. Alkofer, M. Klok, A. Krassnigg, C. Roberts, et al., *Nucl. Phys.* **A755**, 298–302 (2005).

27. J. J. Kelly, *Phys. Rev. C* **66**, 065203 (2002).
28. G. A. Miller, *Phys. Rev. Lett.* **99**, 112001 (2007).
29. G. A. Miller, and J. Arrington, *Phys. Rev.* **C78**, 032201 (2008).
30. G. A. Miller, and J. Arrington, *Int. J. Mod. Phys.* **E18**, 1809–1824 (2009).
31. G. A. Miller, and M. R. Frank, *Phys. Rev.* **C65**, 065205 (2002).
32. S. Boffi, et al., *Eur. Phys. J. A* **14**, 17 (2002).
33. A. V. Belitsky, X.-d. Ji, and F. Yuan, *Phys. Rev. Lett.* **91**, 092003 (2003).
34. S. J. Brodsky, J. R. Hiller, D. S. Hwang, and V. A. Karmanov, *Phys. Rev. D* **69**, 076001 (2004).
35. J. P. Ralston, and P. Jain, *Phys. Rev. D* **69**, 053008 (2004).
36. G. A. Miller, *Phys. Rev.* **C68**, 022201 (2003).
37. A. V. Belitsky, X.-d. Ji, and F. Yuan, *Phys. Rev. D* **69**, 074014 (2004).
38. C. E. Carlson, and M. Vanderhaeghen, *Phys. Rev. Lett.* **100**, 032004 (2008).
39. S. Riordan, et al., *Phys. Rev. Lett.* **105**, 262302 (2010).
40. G. Cates, C. de Jager, S. Riordan, and B. Wojtsekhowski, *Phys. Rev. Lett.* **106**, 252003 (2011).
41. I. Cloet, G. Eichmann, B. El-Bennich, T. Klahn, and C. Roberts, *Few Body Syst.* **46**, 1–36 (2009).
42. I. C. Cloet, and G. A. Miller (2012), [arXiv:1204.4422](#).
43. J. Lachniet, et al., *Phys. Rev. Lett.* **102**, 192001 (2009).
44. J. Dudek, R. Ent, R. Essig, K. Kumar, C. Meyer, et al. (2012), [arXiv:1208.1244](#).
45. G. Ron, et al., *Phys. Rev. Lett.* **99**, 202002 (2007).
46. J. Bernauer, et al., *Phys. Rev. Lett.* **105**, 242001 (2010).
47. D. Borisjuk, and A. Kobushkin, *Phys. Rev. C* **75**, 038202 (2007).
48. P. G. Blunden, W. Melnitchouk, and J. A. Tjon, *Phys. Rev. C* **72**, 034612 (2005).
49. P. G. Blunden, and I. Sick, *Phys. Rev. C* **72**, 057601 (2005).
50. J. Arrington, *Phys. Rev. Lett.* **107**, 119101 (2011).
51. J. Bernauer, et al., *Phys. Rev. Lett.* **107**, 119102 (2011).
52. P. J. Mohr, B. N. Taylor, and D. B. Newell (2012), [1203.5425](#).
53. I. Sick, *Phys. Lett.* **B576**, 62–67 (2003).
54. R. Pohl, et al., *Nature* **466**, 213–216 (2010).